A review on behavior, material properties and finite element simulation of concrete tunnel linings under fire

A Review on Behavior, Material Properties and Finite Element Simulation of Concrete Tunnel Linings under Fire

[1]Zobaer Saleheen, [2]*Renga Rao Krishnamoorthy, [3]Ali Nadjai

[1] School of Civil Engineering, College of Engineering, Universiti Teknologi MARA (UiTM), Malaysia,
[2] Smart Manufacturing Research Institute (SMRI), Universiti Teknologi MARA (UiTM), Malaysia,
[3] FireSERT, Ulster University, United Kingdom
[1] shauravce100@gmail.com, [2]*rao@uitm.edu.my, [3] a.nadjai@ulster.ac.uk

Corresponding author – Smart ManufacturingResearch Institute (SMRI), Universiti Teknologi MARA (UiTM), 40450, Shah Alam, Malaysia. Tel: +603 5543 6426 Fax: +603 5543 5275 e-mail: rao@uitm.edu.my

Abstract: Rigorous understanding of tunnel fire attributes and behavior of concrete at elevated temperatures are indispensable for conducting a numerical simulation of tunnel linings exposed to fire. One of the main feats of tunnel fires is, unlike cellulose fires, temperature of these fires quickly ascends to its zenith, which is higher than conventional cellulose fire temperature. Higher peak temperature in conjunction with rapid heating rate causes spalling in the tunnel linings, which is triggered by excess vapor pressure in concrete pores generated from evaporation of moisture in concrete. Apart from vaporization of moisture, multiple simultaneous physiochemical processes (dehydration/hydration, desorption/sorption, α-β transformation of quartz, decarbonation) take place in concrete when it gets heated. Modelling of a tunnel fire using a commercial finite element tool without taking into account of these physiochemical processes and latent energy associated with the phase changes will result in inaccurate prediction of the results. Thus, the behavior of concrete tunnel liners in extreme fire conditions and relevant material parameters required for numerical simulation are presented in this paper.

1. Introduction

The oldest recorded tunnel fire occurred in 1842 at Mendon, France which caused the death of at least 150 peoples (Beard & Carvel, 2005). Over the past few decades, Europe has experienced several major fires in tunnels which resulted in tremendous loss of life, disruption of services and a notable damage of tunnel liners. The Channel tunnel which connects the UK to European mainland has suffered three major fire

incidents (1996, 2006 and 2008) in its life time. Even though these three fires did not have any fatalities, they caused a severe damage in the tunnel linings (Tarada & King, 2009). After the occurrence of several other major tunnel fires in European mainland such as Mont Blanc (1999), Lanzier (1999), Tauern (1999) and Gotthard (2001), the European Union (EU) initiated actions to investigate tunnel fire safety issues which resulted in production of two documents stating the minimum fundamental safety requirements for tunnels subjected to fire (Cafaro & Bertola, 2010; Tarada & King, 2009).

Carvel (Beard & Carvel, 2005) stated that according to French, German, Swiss and Italian statistics, accidents have higher probability of occurrence in open roads than in tunnels. The main reasons for the lower number of accidental fires in road tunnels include fewer sharp bends or intersections, less susceptibility to weather variations and additional cautiousness of drivers in tunnels. For railway tunnels, the majority of fires was appeared to have started from some sort of electrical or mechanical failures; only a minor fraction of the fires was caused by human errors. Most of the disastrous fire incidents in either railway or roadway tunnels were caused by HGVs (Heavy Good Vehicles). Statistics showed that one to three number of major fires will be caused out of a thousand million HGVs (Beard & Carvel, 2005). However, small cross-sectional dimensions and unfavorable escape opportunities in the tunnels have made the consequences of fires in tunnels far greater than in open road/railway tracks. The catastrophic consequences of tunnel fire can be perceived by the following historical fire incidents. In 1984, the Summit tunnel fire was caused by a train derailment, lasted for four days. The tunnel was reopened for public eight months after the fire. Similar scenario was observed in the Channel tunnel fire (1996) which ceased all the operations of the tunnel for about six months. One hundred and fifty five lives were lost when a train caught fire at the Kaprun funicular (2000), which resulted in its permanent closure (Khorasani et al., 2018).

These fire incidents have stirred studies looking into tunnel fires which led to six directions (Qiao et al., 2019) namely, (i) fire detection/alarm, (ii) evacuation, (iii) ventilation, (iv) fire extinguishment systems, (v) rehabilitation/retrofitting and (vi) fire resistance and damage evaluation of linings. As almost all of the previous major tunnel fires caused notable damage in the tunnel lining, amidst these six categories of tunnel

research, fire resistance and damage evaluation of tunnel liners is an important area to focus on. Researchers have taken different approach towards fire resistance of tunnel linings. For example, Caner et al.(2009), Lai et al. (2014), Yasuda et al. (2004) etc. have taken the experimental approach, whilst Kumar et al. (1989), Kodur & Dwaikat (2008), Khoury (2000) have taken prescriptive or performance based numerical approach. Since conducting experimental fire tests on tunnel linings are large-scale destructive tests which require a great deal of resources and money, lately numerical analysis has become a prevailing and popular tool for this kind of studies. However, performing a numerical simulation of a tunnel fire requires comprehensive understanding of fire characteristics, thermal, hydral and mechanical response of materials during fire. Despite the availability of abundant researches in this area, diverse approaches of different researchers and scarcity of the experimental data required for modelling has made it quite difficult for a new researcher to perform a numerical simulation of a tunnel lining exposed to fire.

Thereby this paper intends to provide a comprehensive understanding of the fire scenario, behavior of concrete at elevated temperatures together with the material properties that are required for basic and advanced level of modelling. Since these information are available in scattered documents, presenting them in a single paper would ease the modelling of heated concrete for tunnel fire researchers.

2. Fire Curves

Using a standard temperature curve that properly represents the tunnel fire scenario is of foremost priority while performing a numerical simulation. The cellulosic fire curves (e.g., ISO 834 or BS 476), are based on the burning of wood, paper or fabric. It was being used for many years until it became apparent that the fires in tunnels are of higher intensity and reach higher temperatures. Furthermore, the ISO 834 fire curve does not depicts burning of petrol or chemicals (Khoury, 2000; Lönnermark, 2005; Promat, 2008). Thus, the Hydrocarbon (HC) fire curve which was developed in the 1970's for the petrochemical and offshore industries was adopted for tunnels. While the ISO 834 fire curve reaches 842°C in 30 minutes, HC curve rises to 1050°C within 5 minutes. However, after noticing the rapid ascension of temperature in Mont Blanc (1999) and Tauern (1999) tunnels, the French government published a new regulation for tunnel fire safety

in August of 2000 where they introduced an increased Hydrocarbon curve, which is widely known as HCM (Modified Hydrocarbon) or HC_{inc} fire curve (Taillefer et al., 2013). Maximum temperature of 1100°C of HC curve was increased to 1300°C for the French HCM curve.

Meanwhile other countries started developing their own standard fire curves. In 1979, after a devastating accidental fire in the Velsar tunnel, TNO center of Fire Safety of Netherlands (TNO, 1998) proposed the RWS *(Rijkswaterstatt)* fire curve which simulates the burning of a $50m^3$ petrol tanker of 300MW fire for two hours. The RWS curve was initially proposed on the Dutch experience of tunnel fires which was supported by the full scale fire tests conducted in Sweden's Runehamar tunnel under UPTUN project of European Commission (EFNARC, 2006; Jong, 2020; Lönnermark, 2005). RWS curve is by far the most extreme fire curve being used, where the temperature quickly ascends to 1200°C and reaches up to 1350°C at 60 minutes within 120 minutes of total fire exposure.

The German Ministry of Transport developed RABT fire curve in 1985 for both railway and highway tunnels as a part of the Eureka project (Kim et al., 2019; Lönnermark, 2005). Temperature of RABT curve rises to 1200°C within 5 minutes of fire exposure at a sharp gradient of 240°C/min, then it remains constant at 1200°C until 30 minutes and 60 minutes respectively for highway and railway tunnels. Unlike other fire curves, RABT curve has a cooling branch which takes 110 minutes to plunge from 1200°C to ambient temperature.

Figure 1 shows five different temperature-time curves that are currently being used to simulate tunnel fire in different countries. Whilst, RWS (1350°C), HCM (1300°C) and RABT (1200°C) curves have high temperatures and the rapid heating rates, the lowest heating rate and the lowest temperature was found in IS 834. According to PIARC, the highest gas ceiling temperature due to burning of cars and buses/vans will be 400°C and 700°C respectively. Considering the above-mentioned fact, PIARC has recommended to use ISO 834 (one hour) temperature curve for tunnel fire cases where only cars or vans may set ablaze. On the contrary, temperature during HGV or petroleum tanker fire will arise up to 1350°C or 1400°C, so in those cases PIARC has recommended to use HCM or RWS fire curves for two hours (ITA, 2004; Lönnermark,

2005). As per PIARC, the fire resistance of tunnels should be set in such a manner that they are never subjected to progressive collapse due to fire, damage in liners may be accepted to a certain extent keeping in mind that local damage in linings will not cause a progressive failure. These recommendations by PIARC was found to be in agreement with ITA (International Tunneling Association) (ITA, 2004).

3. Behavior of Concrete at Elevated Temperatures

Concrete is mainly composed of two ingredients: hydrated cement paste and aggregates. Changes in concrete properties at elevated temperatures take place due to three factors, namely, physiochemical reactions of hydrated cement paste, aggregates and the thermal incompatibility between those. Portland cement clinkers of hydrated cement paste (i.e. Calcium Silicate Hydrate (CSH), where, C for CaO, S for SiO_2, H for H_2O) mainly consists of 45% of tricalcium silicate (C_3S), 25% of β dicalcium silicate (C_2S) and some other compounds like C_3A (A for Al_2O_3), C_4AF (F for Fe_2O_3), calcium sulfate etc. (Fernandes et al., 2017; Harmathy, 1970). The main function of CSH is to bind the aggregates together. It is a porous medium which consists of pores and a solid skeleton. Although there are some poorly distinguishable A-, F-containing hydrates and anhydrous residues of cement, the calcium silicate hydrate (CSH) is generalized as the solid skeleton constituent of concrete for modelling purposes (Harmathy, 1970; Khoury et al., 2002). Water within the pores (outside of the hygroscopic region) is known as a capillary or free water. There are two types of water that is present within the hygroscopic region, those are (i) adsorbed water, which is physically bound to the solid skeleton surfaces by the electrochemical forces and (ii) chemically bound water, that is a part of the solid skeleton (CSH).

3.1. Influence of Temperature on Hydrated Cement Paste

Khoury (2000), Harmathy (1970; 1973) and several other researchers have studied the physiochemical changes of concrete at different temperatures. Figure 2 shows a graphical representation of the processes associated with heating of concrete. Figure 2 shows that the hydrothermal reactions of concrete start at around 100°C. At first, the capillary/free water in concrete pores and adsorbed water starts to evaporate. Even though by 100°C, all of the free water in concrete pores gets evaporated in small elements, sometimes

for larger elements or denser concretes, some of the free water gets driven towards the lower thermal gradient (Khoury et al., 2002). When all of the capillary water of concrete is evaporated then it is only saturated with physically adsorbed water and chemically bound water, that point is known as the SSP (solid saturation point). Water from the calcium silicate hydrate (i.e. chemically bound water) starts to get released above 80°C but it becomes significant at around 110°C (Khoury et al., 2002; Millard & Pimienta, 2019). Consequently, the solid skeleton of concrete is subjected to a mass loss. Mass loss of the solid skeleton is noted again at about 500°C, when calcium hydroxide gets disintegrated into calcium oxide and water (Khoury et al., 2002). Since mechanical properties of concrete are more dependent on CSH than CH, deterioration of mechanical properties is more prominent during the loss of chemically bound water and physically bound water. Therefore, evaporation of capillary or free water does not have any effect on strength of concrete.

3.2. Influence of Temperature on Aggregates

Thermal properties (e.g., conductivity, specific heat, etc.), stability and expansion of concrete is dependent on the type and microstructure of aggregates being used in the concrete. Siliceous aggregates containing quartz goes through the transformation from α to β crystalline at 573°C, which causes endothermic reactions during heating and volumetric expansion of 5.7% (Fernandes et al., 2017; Millard & Pimienta, 2019). Endothermic reaction of aggregates hinders the heat transfer of concrete during fire. Similar trend of endothermic reactions also takes place in calcareous aggregates above 650°C during decarbonation of calcium carbonate ($CaCO_3$) into calcium oxide (CaO) and carbon dioxide (CO_2) (Fernandes et al., 2017; Millard & Pimienta, 2019).

3.3. Influence of Temperature on Transition Zone

The 50μm thick interfacial bridge between aggregates and hydrated cement paste is known as the transition zone (Fernandes et al., 2017). Due to the fissures and voids in the transition zone, transfer of stresses within the concrete gets hindered, thereby it is referred as the weak link of concrete. This region of concrete, which

significantly reduces its stiffness, has microcracks even before any loads are applied (Mehta & Monteiro, 2014).

As shown in Figure 3, expansion of aggregates and calcium silicate hydrate occurs at different rate when concrete is subjected to elevated temperatures. However, during the moisture loss of concrete due to evaporation of capillary water and dehydration of chemically bound water, CSH undergoes severe shrinkage. On the other hand, expansion of the aggregates continues to escalate. This phenomenon results in cracking of concrete, as transition zone is the weakest link of concrete due to its fragility, the cracks are initiated from this zone.

4. Properties of Concrete at Elevated Temperatures

Evaluating fire performance of concrete by means of numerical simulations has become quite popular over the last decades because these methods are much less time consuming and less expensive than the experimental fire tests (CEB-FIP, 2007). The fundamental behavioral changes of concrete when it is exposed to high temperature can be expressed in terms of thermal, mechanical and deformation properties of concrete. Profound understanding of these properties along with the spalling characteristics are vital in order to formulate a mathematical model of fire performance of concrete tunnel lining (V. K. R. Kodur et al., 2004, 2009). Conventional properties of concrete at ambient temperature are hardly useful for evaluating fire performance of concrete. All of the above-mentioned properties are reliant on chemical composition and characteristics of concrete and reinforcing steel. Since these properties vary with temperature, they are expressed as functions of temperature (V. K. R. Kodur & Harmathy, 2016). Due to temperature induced moisture migration and physiochemical reactions, these temperature dependent properties of concrete are more intricate than those of reinforcing steel. Thereby, the main focus of this section is on the influence of temperature on different properties of concrete.

Manifestation of superior fire resistance of concrete has led to its worldwide application in building and infrastructure industries where fire safety is one of the foremost priority (V. K. R. Kodur & Khaliq, 2011). Now-a-days a wide variety of concretes are being used in the industry, which can be categorized based on

their weight, strength, performance, presence of fibers etc. Since properties of concrete are greatly influenced by the types of aggregates used in the mixture, fire researchers have further subdivided concrete into siliceous aggregate concrete and calcareous aggregate concrete, based on the composition of the principal aggregate (V. K. R. Kodur, 2014).

Over the past few decades, a great deal of research has led to the development of improved concrete mixes like HSC (High Strength Concrete), SCC (Self Consolidating Concrete), UHPC (Ultra high-performance concrete), etc. (V. K. R. Kodur & Khaliq, 2011). Even though these concretes exhibit enhanced structural performance and durability which results in economic design, the fire performance of these concretes are considerably inferior to those of NSC (Normal Strength Concrete) (V. K. R. Kodur & Sultan, 2003, 1998)

4.1. Thermal Properties

Prediction of heat transfer and temperature distribution of fire exposed concrete is formulated with help of the thermal properties, which includes conductivity, specific heat, diffusivity and mass loss.

4.1.1. Thermal Conductivity of Concrete

Thermal conductivity manifests a material's capability to conduct heat (Cengel, 2002). Conventionally it is expressed as λ and is measured in W/m/K. Conductivity of concrete can be measured by either using steady state or transient test methods (Bazant & Kaplan, 1996). Conductivity is significantly influenced by moisture migration and physiochemical changes that take place in concrete during heating. Due to these phenomena, using steady state test methods it results in erroneous prediction of thermal conductivity in moist concrete (Shin et al., 2002). Owing to these facts, researchers prefer to use the transient test methods over the steady state. Numerous techniques are available for measuring thermal conductivity, results of which may vary depending on the method being employed (Khaliq, 2012). Among these methods, guarded heat flow (ASTM E1530, 2011) and hot wire (ASTM C1113, 2009) methods are mostly used for measuring conductivity of concrete.

Figure 4 shows the variation of thermal conductivity reported by Eurocode 2 (1996) and range of experimental data provided by Shin et al. (2002), Harmathy & Allen (1973), Lie (1992) and Kodur & Sultan (2003). Bazant & Kaplan (1996) stated that thermal conductivity of concrete at room temperature is between 1.4 to 3.6 W/m/K. This fluctuation can be ascribed to the mix proportion, water cement ratio as well as the type of the principal aggregate being used in the concrete. For example, concretes composed of siliceous aggregate usually demonstrate greater thermal conductivity than calcareous aggregate concrete. Thereby, Eurocode 2 (1996) has recommended to use the upper bound values for siliceous aggregate and lower bound values for calcareous aggregate concrete. However, conductivity for all types of concrete declines with increasing temperature due to the moisture loss and the change of permeability at elevated temperatures.

4.1.2. Specific Heat of Concrete

Specific heat is the energy required to increase temperature of a unit mass of a material by 1°C, which is denoted as C_p and measured in J/kg/K. Specific heat of concrete can be determined by quite a few test methods. Up until 1980's the adiabatic calorimetry was the primary method to determine specific heat of concrete.

However, for the past few decades, differential scanning calorimetry (DSC) (ASTM E1269, 2011) has been used in this regard (V. K. R. Kodur, 2014; V. K. R. Kodur & Harmathy, 2016). As DSC provides best results up to 600°C, Harmathy & Allen (1973) used DTA (high temperature differential thermal analyzer) for temperature above 600°C. With the help of DuPont 910 DSC, Harmathy & Allen (1973) developed calorimetric curves for different type of concrete mixes. He demonstrated that due to the phase changes (e.g., evaporation, dehydration of CSH into β-CS and β-C_2S, disassociation of $Ca(OH)_2$ into CaO and water, etc.), a certain amount of additional energy is absorbed by the system, which is known as the latent energy of phase change. As the latent heat/energy due to these phase changes had a significant contribution to the apparent specific heat of concrete, accuracy for ascertaining the sensible heat contribution in the apparent specific heat using DSC technique got reduced (it can be as low as ±20%) (V. K. R. Kodur, 2014; V. K. R.

Kodur & Harmathy, 2016). Figure 5 illustrates the specific heat of concrete reported by Lie (1992), Harmathy & Allen (1973), Eurocode 2 (1996), Shin et al. (2002) and Kodur & Sultan (2003). Specific heat of concrete at room temperature (only the sensible heat contribution) fluctuates between 840 to 1800 J/kg/K, depending on the type of aggregates (V. K. R. Kodur, 2014). Generally, the specific heat increases with increasing temperature, gradient of which is relatively mild. However, two or three sharp peaks in the specific heat are detected due to the physiochemical reactions of concrete at elevated temperatures. During the physiochemical reactions most of the heat is consumed by the system. For example, at around 100-150°C, evaporation of free water takes place which absorbs most of the heat and only a small portion of heat is available to raise the temperature of concrete. Thereby, specific heat concrete increases significantly in this temperature region. Specific heat of concrete increases again at near 400-500°C when the water from hydrated cement paste is dehydrated. Apart from evaporation of the capillary water and dehydration of CSH, aggregates also have significant influence on the specific heat of concrete. Transformation of quartz in siliceous aggregates takes place after around 500°C, which causes a slight peak in specific heat. On the other hand, for the carbonate aggregates, the specific heat increases approximately 10 times in 600-800°C temperature range due to decarbonation.

4.1.3. Mass Loss

When concrete is heated, it is subjected to the mass loss due to the removal of moisture. Conventionally it is measured by TGA technique (ASTM E1868, 2010).

Figure 6 illustrates rate of mass loss of different types of concrete reported by Hu et al. (1993), Kodur & Sultan (2003) and Hachemi et al. (2014). Mass loss of concrete was observed to be heavily influenced by the type of aggregate. The percentage of mass loss for both kind of aggregate is insignificant before 600°C, whereas, siliceous aggregates was subjected to the minor mass loss beyond 600°C, substantial percentage of mass was lost in calcareous aggregate concrete due to decarbonation of dolomite.

4.2. Mechanical Properties

The parameters that control the mechanical performance of concrete are modulus of elasticity, compressive and tensile strength. Due to the physiochemical reactions of heated concrete, performance of these properties declines with the increasing temperature.

4.2.1. Modulus of Elasticity

At high temperatures, due to the disassociation of CSH and rupture of bonds in the cement paste microstructure, the modulus of elasticity decreases.

Modulus of elasticity of concrete at ambient temperature fluctuates between 5000 to 35000 MPa, depending on the strength, age of concrete, water cement ratio, type of aggregate, etc. Figure 7 demonstrates the loss of elastic modulus of concrete as per Eurocode (1996), Choi et al.(2013), Chang et al. (2006), Lu (1989) (reported in Xiao & König, (2004)), Li & Guo (1993) (reported in Xiao & König, (2004)) and Li & Purkiss (2005). Even though, both NSC and HSC gradually starts to lose its elasticity after 150°C and lose almost 80 to 90 percent by the time it reaches 800°C, the wide range of variation of on experimental test data were found. The deterioration of elasticity of concrete was found to be independent of the type of aggregate used in the concrete.

4.2.2. Compressive Strength & Tensile Strength

Figure 8 illustrates the relative compressive strength of concrete given by Eurocode 4 & 2 (2005; 2004), Choi et al. (2013), Li & Purkiss (2005), Chang et al. (2006), and Hertz (2005). It shows that up to 300°C, temperature has minimal effect on the compressive strength of concrete. Concrete only loses 10 to 15 percent of its compressive strength by that temperature. However, from 300°C to 800°C, almost 80 to 90 percent of the concretes compressive strength diminishes.

Similarly Figure 9 demonstrates the loss of tensile strength with temperature given by Eurocode 2 (2004), Bazant & Chern (1987), Li & Guo (1993) (reported in Xiao & König, (2004)), Chang et al. (2006). Among

the above mentioned models, Eurocode 2 (2004) provides the most conservative model where the tensile strength of concrete diminishes by 600°C.

4.2.3. Stress-Strain Relationship

The mechanical response of concrete is conventionally described by the stress strain relationships. As shown in Figure 10 and Figure 11, the linear steep slope of stress strain curve starts to get mild with increasing temperature. This can be attributed to the loss of compressive strength and ductility of the concrete at elevated temperatures. As a consequence, the strain starts to increase with increasing temperature. The peak strain of concrete at 500°C was found to increase 4 to 10 times than of room temperature for both 40 MPa and 26 MPa concretes.

5. Modelling of Heated Concrete

Fire performance of a structure can either be evaluated by conducting experimental fire tests or numerical simulations. Since, experimental tunnel fire tests are large scale destructive tests which are quite expensive and require plenty of resources, lately numerical simulations have become a powerful and prevailing tool for this kind of studies. Different approaches towards numerical simulation of concrete tunnel linings under fire have been adopted by different researchers. The accuracy of the numerical simulations is dependent on the representations of complex behaviour of concrete under fire. Prescriptive approach is the most unambiguous approach available in the industry where normally load bearing capacity of a structure after fire is assessed by employing generalized code provisions (e.g., Eurocode (EN1992-1-2, 1996) or ASCE (Lie, 1992)) which does not take into account of the variations of heating rate or peak temperature that are encountered in the real-life scenarios. Even though prescriptive approach is quite simplistic and easy to carry out, due to poor representation of practical scenario it is not preferred by current researchers. On the other hand, performance-based approach evaluates the response of a structure or part of a structure during real life fire scenarios. Nevertheless, precision of the performance-based approach is fervently reliant on the scale of modelling and level of description of complex physiochemical reactions of heated concrete. Based on the above-mentioned factors, the performance-based modelling can be characterized in two types,

namely, engineering modelling (i.e., thermo-mechanical analysis) and advanced modelling (i.e., coupled thermo-hydro-chemo-mechanical analysis framework).

5.1. Engineering Modelling

Thermo-mechanical analysis which produces numerical results of reasonable accuracy with acceptable computational costs for engineering purposes is known as engineering modelling. Here, complex physiochemical processes of heated concrete are simplified up to an extent, given that those simplifications result in a satisfactory deviation from the experimental scenario. In the thermo-mechanical framework, analysis is done in two consecutive steps. At first, temperature field is calculated by means of the thermal properties (thermal conductivity, specific heat, mass loss) then evolution of the temperature is coupled to mechanical analysis with the help of thermal strain and mechanical properties at elevated temperature (Millard & Pimienta, 2019). Variation of mechanical properties (modulus of elasticity, compressive strength, coefficient of thermal expansion, etc.) of concrete at different temperature available in different codes and studies (e.g. (Y. F. Chang et al., 2006; Harmathy & Allen, 1973; L. Y. Li & Purkiss, 2005; ÖBV, 2013)), are being used in the thermomechanical analysis framework to evaluate the temperature effects on the tunnels. Different researchers have opted different techniques for thermo-mechanical numerical simulation of tunnel linings subjected to elevated temperatures. Qiao et al. (2018, 2019) have suggested a theoretical method for assessment of the damage and safety of concrete tunnel linings exposed to long duration fire by employing laplace transform and series solving method for ordinary differentiation equations. Yan et al. (2020) was focused on developing a theoretical model of tunnel segments based on multilayer curved beam theory while incorporating progressive thermal damage in the model. Although Qiao et al. (2018, 2019) and Yan et al. (2020) have chosen to develop their own analytical model, researchers like Zhang et al. (2019) and Bernardi et al. (2020) have used commercially available software such as Abaqus CAE to evaluate the thermo-mechanical response of concrete tunnel linings.

Although, the physiochemical reactions (e.g., moisture evaporation, dehydration, α-β transformation, decarbonation, etc.) are not explicitly modelled in this framework, these phenomena are implemented

indirectly through incorporating the latent energy in the specific heat of a material. Nevertheless, the main drawback of this framework is, it does not take into account of the variation of pore pressure due to the differential thermal gradient. The increase of vapor pressure due to moisture vaporization is one of the root causes of spalling. Since the thermo-mechanical framework does not take into account of the variation of pore pressure, researchers using thermo-mechanical analysis have incorporated spalling using different techniques. For instance, Sakkas et al. (2019) have conducted in situ fire tests on concrete tunnel and recorded the rate of fire induced spalling which was used to perform a numerical simulation using FLAC3D software to evaluate the structural integrity of the tunnel and nearby structures.

Some researchers (e.g Savov et al.(2005), Chang et al. (2016), Choi et al., (2013), Saleheen & Krishnamoorthy (2020), etc.) have simulated spalling by selecting a critical temperature, above which the concrete is considered as damaged or spalled. This method is known as the element elimination method which has been adopted for tunnel fire by Chang et al. (2016) and Choi et al., (2013) and was later on modified by Saleheen & Krishnamoorthy (2020).

5.2. Advanced Modelling

In order to overcome the above-mentioned limitations of the conventional thermo-mechanical framework, an advanced modelling technique is proposed in the literature, which is based on thermo-hydro-chemo-mechanical (THCM) coupling of concrete. In the THCM framework, concrete is regarded as a porous medium, pores of which are partially filled with gas and water (Millard & Pimienta, 2019). Proper coupling of TCHM requires rigorous understanding and proper representation of properties of fluids that fills the pores of concrete. The movement of moisture is strongly dependent on the permeability and diffusion characteristics of concrete, which is sensitive of the change of porosity of concrete at high temperatures. Since, these properties are heavily influenced by the temperature, they are generally expressed as functions of temperature.

5.2.1. Porosity

Due to the dehydration of cement paste (CSH) the total pore volume of concrete increases, which can be attributed to the increase of porosity in heated concrete. Schneider & Herbst (1989) studied the porosity of different types of concrete with increasing temperature. Based on those works, Gawin et al. (1999) used the least square method to propose a linear relationship of porosity as a function of temperature, which is as follows

$$\varphi_T = \varphi_0 + A_\varphi (T - T_0) \quad (1)$$

where φ_0=porosity of concrete at room temperature T_0, A_φ is a constant which is dependent on the type of concrete (refer to Table 1)

Table 1 Porosity coefficients (Gawin et al., 1999)

Coefficients	**Silicate Concrete**	**Limestone Concrete**	**Basalt Concrete**
φ_0	0.060	0.087	0.0802
$A\varphi$	0.000195	0.000163	0.00017

5.2.2. Permeability

The intrinsic permeability of a material represents the geometrical connectivity of the porous network, which is independent of the fluid filling the pore. Thereby, the term relative permeability is introduced which takes into account of the penetration of gas, water and their coexistence in the porous network (Millard & Pimienta, 2019). Permeability of concrete was observed to be heavily influenced by temperature and gas pressure of heated concrete. Based on the experimental works of Schneider & Herbst (1989), Gawin et al. (1999) proposed the following equation which shows the relationship of intrinsic permeability with temperature and gas pressure.

$$k = k_0 \times 10^{A_k(T-T_0)} \left(\frac{P_g}{P_0}\right)^{B_k} \quad (2)$$

where A_k and B_k are constants which depend on the characteristics of concrete, k_0 is the intrinsic permeability of concrete at reference temperature T_0= 293.15 K and reference gas pressure P_0= 101325 Pa.

Equation (3) shows relative permeability of water for soil mechanics given by van Genuchten (1980), which was later on validated by Savage & Janssen (1997) for modelling of moisture movement in unsaturated Portland cement concrete.

$$k_{rl} = \sqrt{S_l}\left(1 - \left(1 - S_l^{\frac{1}{A}}\right)^A\right)^2 \quad (3)$$

where S_l=degree of saturation, A=exponent of capillary pressure curve. The relative permeability of water in terms of relative humidity given by Gawin et al. (1999) is presented in equation (4)

$$k_{rl} = \left[1 + \left(\frac{1 - RH}{0.25}\right)^{B_l}\right]^{-1} \times S^{A_l} \quad (4)$$

where RH is relative humidity, A_l and B_l are constants whose range is <1,3>. Equation (5) shows the gas relative permeability developed by Luckner et al. (1989)

$$k_{rg} = \sqrt{1 - S}\left(1 - S^{1/m}\right)^{2m} \quad (5)$$

where m is a constant

5.2.3. Diffusivity

The vapor diffusion process is heavily affected by the sophisticated pore structure of concrete. Due to the complex pore structure of concrete and lack of experimental data available the tortuosity factor, τ and the constrictivity factor δ was introduced in the diffusion equation. Whereas, tortuosity factor takes into account of the increase in average path of the diffusing particles, constrictivity factor take into consideration of the constriction of pores due to different size of connected particles in the pore space.

The effective diffusion coefficient of water vapor in terms of temperature and gas pressure in the partially saturated concrete pore given by Atkinson & Nickerson (1984) is:

$$D_{eff} = D\frac{\tau}{\delta^2}\varphi(1 - S_l) \quad (6)$$

where τ= tortuosity factor, δ= constrictivity factor, approximate value of τ and δ is 0.5 and 3 respectively (Fadul, 2017). φ=porosity of concrete, S_l= Saturation of concrete and D (m^2/s). The diffusion coefficient of water vapor in free air given by Cengel (2002),

$$D = 1.87 \times 10^{-5}\frac{(273.15 + T)^{2.072}}{P_g} \quad (7)$$

where T is the temperature in Celsius, P_g is the vapor pressure in Pa

5.2.4. Advanced Modelling Approaches

In this framework, mass energy and momentum balance equations are coupled in such a manner that the physiochemical aspects of heated concrete (e.g., evaporation, hydration-dehydration, α-β transformation of quartz, decarbonation of calcium carbonate) are taken into account. Even the change in macroscopic properties (e.g., porosity, permeability) with temperature is also incorporated in this framework. Modelling of concrete as a porous medium in THCM framework can be done whether by adopting phenomenological approach or mechanistic approach.

Finite element simulation of heat and mass transfer in phenomenological approach (Abdel-Rahman & Ahmed, 1996; Bazant & Thonguthai, 1979; England & Khoylou, 1995) is implemented by diffusion type differential equations with moisture content and temperature dependent coefficients. These coefficients are derived from experimental tests by employing a backward problem solution technique. In this approach, various physiochemical phenomena are lumped into one process and the phase change associated with those processes are ignored.

Mechanistic approach (Bazant & Kaplan, 1996; Consolazio et al., 1998; Gawin et al., 1999, 2002; Ulm, Acker, et al., 1999; Ulm, Coussy, et al., 1999) is more complex than phenomenological ones from mathematical perspective. Contrary to the phenomenological approach, the coefficients used in this approach have a physical significance. This model is derived from the macroscopic balance equations (e.g. mass balance equation, enthalpy balance equation, etc.) written for each component of the medium, which are then averaged in the space applying special averaging operators (Zeiml et al., 2008). With recent developments in the commercially available finite element packages, researchers like Yao et al. (2020), V. Kodur & Banerji (2021), etc. have used Abaqus, FORTRAN or MATLAB in order to conduct numerical simulation to evaluate effects of fire in concrete in the THCM framework.

6. Summary

The physiochemical changes associated with the heated concrete affect the properties of concrete such as elasticity or strength. The deterioration of properties along with the additional pore pressure development of concrete introduce complexities, such as spalling. Furthermore, many of these properties are temperature dependent and sensitive to testing (method) parameters such as heating rate, strain rate, temperature gradient, and so on. Based on the information presented in this paper, it is evident that high temperature properties of concrete are crucial for modeling fire response of reinforced concrete structures. A good amount of data exists on high temperature thermal and mechanical properties of concrete, which were broadly represented in this paper along with the behavior of heated concrete. Further details related to the specific conditions on which these properties were developed can be found in the cited references.

Reference

Abdel-Rahman, A. K., & Ahmed, G. N. (1996). Computational Heat and Mass Transfer in Concrete Walls Exposed to Fire. *Numerical Heat Transfer, Part A: Applications: An International Journal of Computation and Methodology*, *29*(4), 373–395. https://doi.org/10.1080/10407789608913798

ASTM C1113. (2009). *Standard Test Method for Thermal Conductivity of Refractories by Hot Wire (Platinum Resistance Thermometer Technique)*. ASTM International.

ASTM E1269. (2011). *Standard Test Method for Determining Specific Heat Capacity by Differential*

Scanning Calorimetry. https://doi.org/10.1520/E1269-11.2
ASTM E1530. (2011). *Standard Test Method for Evaluating the Resistance to Thermal Transmission of Materials by the Guarded Heat Flow Meter Technique*. ASTM International. https://doi.org/10.1520/E1530-11.2
ASTM E1868. (2010). *Standard Test Methods for Loss On Drying by Thermogravimetry*.
Atkinson, A., & Nickerson, A. K. (1984). The diffusion of ions through water-saturated cement. *Journal of Materials Science*, *19*, 3068–3078. https://doi.org/10.1007/BF01026986
Bazant, Z. P., & Chern, J.-C. (1987). Stress-induced Thermal and Shrinkage Strains in Concrete. *Journal of Engineering Mechanics*, *113*(10), 1493–1511.
Bazant, Z. P., & Kaplan, M. F. (1996). *Concrete at High Temperatures: Material Properties and Mathematical Models*. Longman.
Bazant, Z. P., & Thonguthai, W. (1979). Pore pressure in heated concrete walls : theoretical prediction. *Magazine of Concrete Research*, *31*(107), 67–76.
Beard, A., & Carvel, R. (Eds.). (2005). *Handbook of Tunnel Fire Safety* (2nd ed.). ICE Publishing.
Bernardi, P., Michelini, E., Sirico, A., Rainieri, S., & Corradi, C. (2020). Simulation Methodology for the Assessment of the Structural Safety of Concrete Tunnel Linings based on CFD Fire – FE Thermo-mechanical Analysis : A Case Study. *Engineering Structures*, *225*. https://doi.org/10.1016/j.engstruct.2020.111193
Cafaro, E., & Bertola, V. (2010). Fires in Tunnels : Experiments and Modelling. *The Open Thermodynamics Journal*, *4*, 156–166.
Caner, A., & Böncü, A. (2009). Structural Fire Safety of Circular Concrete Railroad Tunnel Linings. *Journal of Structural Engineering*, *135*(9), 1081–1092. https://doi.org/10.1061/(asce)st.1943-541x.0000045
CEB-FIP. (2007). *CEB-FIP Bulletin 38-Fire Design of Concrete Structures-Materials, Structures and MOdelling*.
Cengel, Y. A. (2002). *Heat Transfer, A Practical Approach* (Second Edi). McGraw-Hill.
Chang, S. H., Choi, S. W., & Lee, J. (2016). Determination of the Combined Heat Transfer Coefficient to Simulate the Fire-induced Damage of a Concrete Tunnel Lining under a Severe Fire Condition. *Tunnelling and Underground Space Technology*, *54*, 1–12. https://doi.org/10.1016/j.tust.2016.01.022
Chang, Y. F., Chen, Y. H., Sheu, M. S., & Yao, G. C. (2006). Residual Stress-Strain Relationship for Concrete after Exposure to High Temperatures. *Cement and Concrete Research*, *36*, 1999–2005. https://doi.org/10.1016/j.cemconres.2006.05.029
Choi, S. W., Lee, J., & Chang, S. H. (2013). A Holistic Numerical Approach to Simulating the Thermal and Mechanical Behaviour of a Tunnel Lining Subject to Fire. *Tunnelling and Underground Space Technology*, *35*, 122–134. https://doi.org/10.1016/j.tust.2013.01.004
Consolazio, G. R., McVay, M. C., & Rish III, J. W. (1998). Measurement and Prediction of Pore Pressures in Saturated Cement Mortar Subjected to Radiant Heating. *ACI Materials Journal*, *95*(5), 526–536. https://doi.org/10.14359/395
EFNARC. (2006). *Specification and Guidelines for Testing of Passive Fire Protection for Concrete Tunnels Linings*. https://doi.org/10.1001/archsurg.1963.01310100072011
EN 1994-1-2. (2005). *Eurocode 4-Design of composite steel and concrete structures- Part 1-2: General rules - Structural fire design Eurocode* (Issue 2005).
EN1992-1-2. (1996). *Eurocode 2-Design of concrete structures - Part 1.2- General Rules-Structural Fire Design*. https://doi.org/10.1680/cien.144.6.23.40607
EN1992-1-2. (2004). *Eurocode 2: Design of concrete structures - Part 1-2: General rules - Structural fire design Eurocode*.
England, G. L., & Khoylou, N. (1995). Moisture Flow in Concrete under Steady State non-uniform Temperature States : Experimental Observations and Theoretical Modelling. *Nuclear Engineering and Design*, *156*, 83–107.
Fadul, M. Al. (2017). *Hydro-thermo-mechanical Behavior of Concrete at Elevated Temperatures*. University of Central Florida.

Fernandes, B., Gil, A. M., Bolina, F. L., & Tutikian, B. F. (2017). Microstructure of Concrete Subjected to Elevated Temperatures: Physico-chemical Changes and Analysis Techniques. *Revista IBRACON de Estruturas e Materiais*, *10*(4), 838–863. https://doi.org/10.1590/s1983-41952017000400004

Gawin, D., Majorana, C. E., & Schrefler, B. A. (1999). Numerical Analysis of Hygro-Thermal Behaviour and Damage of Concrete at High Temperature. *Mechanics of Cohesive Frictional Materials*, *4*, 37–74.

Gawin, D., Pesavento, F., & Schre, B. A. (2002). Simulation of Damage-Permeability Coupling in Hygro-Thermo-Mechanical Analysis of Concrete at High Temperature. *Communications in Numerical Methods in Engineering*, *18*(2), 113–119. https://doi.org/10.1002/cnm.472

Hachemi, S., Ounis, A., & Chabi, S. (2014). Evaluating Residual Mechanical and Physical Properties of Concrete at Elevated Temperatures. *International Journal of Industrial and Manufacturing Engineering*, *8*(2), 176–181.

Harmathy, T. Z. (1970). Thermal Properties of Concrete at Elevated Temperatures. *ASTM Journal of Materials*, *5*(1), 47–74.

Harmathy, T. Z., & Allen, L. W. (1973). Thermal Properties of Selected Masonry Unit Concretes. *Journal of American Concrete Institute*, *70*, 132–162.

Hertz, K. D. (2005). Concrete Strength for Fire Safety Design. *Magazine of Concrete Research*, *57*(8), 445–453. https://doi.org/10.1680/macr.2005.57.8.445

Hu, X. F., Lie, T. T., Polomark, G. M., & MacLaurin, J. W. (1993). *Thermal Properties of Building Materials at Elevated Temperatures*. Internal Report - 643 , Institute for Research in Construction, Natrional Research Council Canada.

ITA. (2004). *International Tunneling Association, Guidelines for Structural Fire Resistance for Road Tunnels*. https://linkinghub.elsevier.com/retrieve/pii/S0886779804000021

Jong, M. De. (2020). *History of the RWS Fire Curve*. https://www.linkedin.com/pulse/history-rws-fire-curve-micha-de-jong

Khaliq, W. (2012). *Performance Characterization of High-Performance Concretes Under Fire Conditions*. Michigan State University.

Khorasani, N. E., Billittier, J., & Stavridis, A. (2018). Structural Performance of a Railway Tunnel under Different Fire Scenarios. *2018 Joint Rail Conference, JRC 2018*, 1–8. https://doi.org/10.1115/JRC2018-6169

Khoury, G. A. (2000). Effect of Fire on Concrete and Concrete Structures. *Progress in Structural Engineering and Materials*, *2*(4), 429–447. https://doi.org/https://doi.org/10.1002/pse.51

Khoury, G. A., Majorana, C. E., Pesavento, F., & Schrefler, B. A. (2002). Modelling of Heated Concrete. *Magazine of Concrete Research*, *54*(2), 77–101. https://doi.org/10.1680/macr.54.2.77.40895

Kim, S., Shim, J., Rhee, J. Y., Jung, D., & Park, C. (2019). Temperature Distribution Characteristics of Concrete During Fire Occurrence in a Tunnel. *Applied Sciences (Switzerland)*, *9*. https://doi.org/10.3390/app9224740

Kodur, V., & Banerji, S. (2021). Modeling the Fire-Induced Spalling in Concrete Structures Incorporating Hydro-Thermo-Mechanical Stresses. *Cement and Concrete Composites*, *117*. https://doi.org/10.1016/j.cemconcomp.2020.103902

Kodur, V. K. R. (2014). Properties of Concrete At Elevated Temperatures. *ISRN Civil Engineering*, *2014*, 429–432.

Kodur, V. K. R., & Dwaikat, M. (2008). A Numerical Model for Predicting the Fire Resistance of Reinforced Concrete Beams. *Cement and Concrete Composites*, *30*(5), 431–443. https://doi.org/10.1016/j.cemconcomp.2007.08.012

Kodur, V. K. R., Dwaikat, M., & Raut, N. (2009). Macroscopic FE model for Tracing the Fire Response of Reinforced Concrete Structures. *Engineering Structures*, *31*, 2368–2379. https://doi.org/10.1016/j.engstruct.2009.05.018

Kodur, V. K. R., & Harmathy, T. Z. (2016). Properties of Building Materials. In *SFPE Handbook of Fire Protection Engineering*. https://doi.org/10.1007/978-1-4939-2565-0

Kodur, V. K. R., & Khaliq, W. (2011). Effect of Temperature on Thermal Properties of Different Types of

High-Strength Concrete. *Journal of Materials in Civil Engineering*, *23*(June), 793–801. https://doi.org/10.1061/(ASCE)MT.1943-5533.0000225

Kodur, V. K. R., & Sultan, M. A. (2003). Effect of Temperature on Thermal Properties of High Strength Concrete. *Journal of Materials in Civil Engineering*, *15*(2), 101–107. https://doi.org/10.1061/(ASCE)MT.1943-5533.0003286

Kodur, V. K. R., & Sultan, M. A. (1998). Structural Behaviour of High Strength Concrete Columns Exposed to Fire. *Procedings of International Symposium on High Performance and Reactive Powder Concrete*, 217–232.

Kodur, V. K. R., Wang, T. C., & Cheng, F. P. (2004). Predicting the Fire Resistance Behaviour of High Strength Concrete Columns. *Cement and Concrete Composites*, *26*(2), 141–153. https://doi.org/https://doi.org/10.1016/S0958-9465(03)00089-1

Kumar, P., & Singh, B. (1989). Thermal stress analysis of underground openings. *International Journal for Numerical and Analytical Methods in Geomechanics*, *13*(4), 411–425. https://doi.org/10.1002/nag.1610130405

Lai, H., Wang, S., & Xie, Y. (2014). Experimental Research on Temperature Field and Structure Performance under Different Lining Water Contents in Road Tunnel Fire. *Tunneling and Underground Space Technology*, *43*, 327–335. https://doi.org/10.1016/j.tust.2014.05.009

Li, L. Y., & Purkiss, J. (2005). Stress-strain constitutive equations of concrete material at elevated temperatures. *Fire Safety Journal*, *40*, 669–686. https://doi.org/10.1016/j.firesaf.2005.06.003

Li, W., & Guo, Z. (1993). Experimental investigation on strength and deformation of concrete under high temperature. *Chin J Build Struct*, *14*(1), 8–16.

Lie, T. T. (Ed.). (1992). *Structural fire protection: ASCE Manuals and Reports on Engineering Practice No. 78.*

Lönnermark, A. (2005). On the Characteristics of Fires in Tunnels. In *Depratement of Fire Safety Engineering, Lund, Suède*.

Lu, Z. (1989). *A Research on Fire Response of Reinforced Concrete Beams*. Tongji University.

Luckner, L., van Genuchten, M. T., & Nielsen, D. R. (1989). A Consistent Set of Parametric Models for the Two-Phase Flow Fluids of Immiscible Fluids in the Subsurface. *Water Resources Research*, *25*(10), 2187–2193.

Mehta, P. K., & Monteiro, P. J. M. (2014). *Concrete: Microstructure, Properties, and Materials* (4th ed.). McGraw-Hill Education. https://www.accessengineeringlibrary.com/content/book/9780071797870

Millard, A., & Pimienta, P. (Eds.). (2019). *Modelling of Concrete Behaviour at High Temperature*.

ÖBV. (2013). *Improved Structural Fire Protection with Concrete for Underground Infrastructure*. Austrian Society for Construction Technology.

Promat. (2008). *Tunnel Fire Protection*.

Qiao, R., Shao, Z., Liu, F., & Wei, W. (2019). Damage Evolution and Safety Assessment of Tunnel Lining Subjected to Long-Duration Fire. *Tunnelling and Underground Space Technology*, *83*(January), 354–363. https://doi.org/10.1016/j.tust.2018.09.036

Qiao, R., Shao, Z., Wei, W., & Zhang, Y. (2018). Theoretical Investigation into the Thermo-Mechanical Behaviours of Tunnel Lining During RABT Fire Development. *Arabian Journal for Science and Engineering*, *44*, 4807–4818. https://doi.org/10.1007/s13369-018-3555-x

Sakkas, K., Vagiokas, N., Tsiamouras, K., Mandalozis, D., Benardos, A., & Nomikos, P. (2019). In-situ Fire Test to Assess Tunnel Lining Fire Resistance. *Tunnelling and Underground Space Technology*, *85*, 368–374. https://doi.org/10.1016/j.tust.2019.01.002

Saleheen, Z., & Krishnamoorthy, R. R. (2020). Numerical Simulation of Spalling and Moisture Evaporation in Concrete Tunnel Linings Exposed to Fire. *Proceedings of the 5th International Conference on Sustainable Civil Engineering Structures and Construction Materials: SCESCM 2020*.

Savage, B. M., & Janssen, D. j. (1997). Soil Physics Principles Validated for Use in Predicting Unsaturated Moisture Movement in Portland Cement Concrete. *ACI Materials Journal*, *94*(1), 63–70. https://doi.org/10.14359/286

Savov, K., Lackner, R., & Mang, H. A. (2005). Stability Assessment of Shallow Tunnels Subjected to Fire

Load. *Fire Safety Journal*, *40*(8), 745–763. https://doi.org/10.1016/j.firesaf.2005.07.004
Schneider, U., & Herbst, H. (1989). Permeabilitaet und porositaet von beton bei hohen temperaturen. *Deutscher Ausschuss Fuer Stahlbeton*, *403*, 23–52.
Shin, K.-Y., Kim, S.-B., Kim, J.-H., Chung, M., & Jung, P.-S. (2002). Thermophysical Properties and Transient Heat Transfer of Concrete at Elevated Temperature. *Nuclear Engineering and Design*, *212*, 233–241.
Taillefer, N., Carlotti, P., Larive, C., Lemerle, C., Avenel, R., & Pimienta, P. (2013). Ten Years of Increased Hydrocarbon Temperature Curves in French Tunnels. *Fire Technology*, *49*(2), 531–549. https://doi.org/10.1007/s10694-012-0259-8
Tarada, F., & King, M. (2009). Structural Fire Protection of Railway Tunnels. *Railway Engineering Conference*, *June*.
TNO. (1998). *Fire Protection for Tunnel (Part1: Fire Test Procedure). TNO Report 1998-CVB-R1161 (rev.1)*.
Ulm, F.-J., Acker, P., & Levy, M. (1999). The '"Chunnel"' Fire. II: Analysis of Concrete Damage. *Journal of Engineering Mechanics*, *125*(March), 283–289.
Ulm, F.-J., Coussy, O., & Bazant, Z. P. (1999). The "Chunnel" Fire. I: Chemoplastic Softening in Rapidly Heated Concrete. *Journal of Engineering Mechanics*, *125*(3), 272–282.
van Genuchten, M. T. (1980). A Closed-form Equation for Predicting the Hydraulic Conductivity of Unsaturated Soils. *Soil Science Society of America Journal*, *44*(5), 892–898. https://doi.org/10.2136/sssaj1980.03615995004400050002x
Xiao, J., & König, G. (2004). Study on Concrete at High Temperature in China - An overview. *Fire Safety Journal*, *39*, 89–103. https://doi.org/10.1016/S0379-7112(03)00093-6
Yan, Z. guo, Zhang, Y., Shen, Y., Zhu, H. hua, & Lu, Y. (2020). A Multilayer Thermo-Elastic Damage Model for the Bending Deflection of the Tunnel Lining Segment Exposed to High Temperatures. *Tunnelling and Underground Space Technology*, *95*. https://doi.org/10.1016/j.tust.2019.103142
Yao, Y., Guo, H., & Tan, K. (2020). An Elastoplastic Damage Constitutive Model of Concrete Considering the Effects of Dehydration and Pore Pressure at High Temperatures. *Materials and Structures*, *53*, 1–18. https://doi.org/10.1617/s11527-020-1450-x
Yasuda, F., Ono, K., & Otsuka, T. (2004). Fire Protection for TBM Shield Tunnel Lining. *Tunneling and Underground Space Technology*, *19*(4–5), 317.
Zeiml, M., Lackner, R., Pesavento, F., & Schrefler, B. A. (2008). Thermo-hydro-chemical Couplings Considered in Safety Assessment of Shallow Tunnels subjected to Fire Load. *Fire Safety Journal*, *43*, 83–95. https://doi.org/10.1016/j.firesaf.2007.05.006
Zhang, Q., Wang, W. Y., Bai, S. S., & Tan, Y. H. (2019). Response Analysis of Tunnel Lining Structure under Impact and Fire Loading. *Advances in Mechanical Engineering*, *11*(3), 1–6. https://doi.org/10.1177/1687814019834473

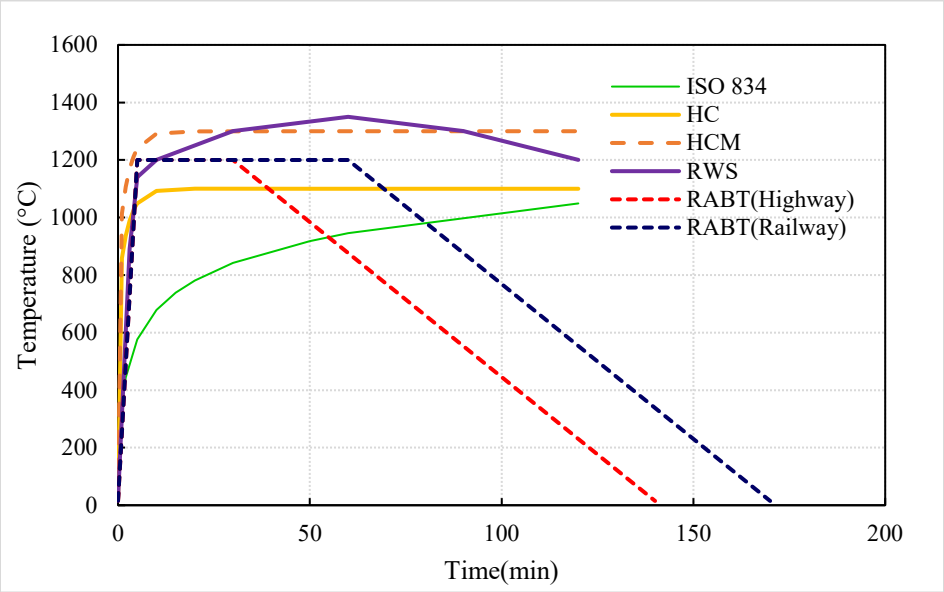

Figure 1 Standard Fire Curves

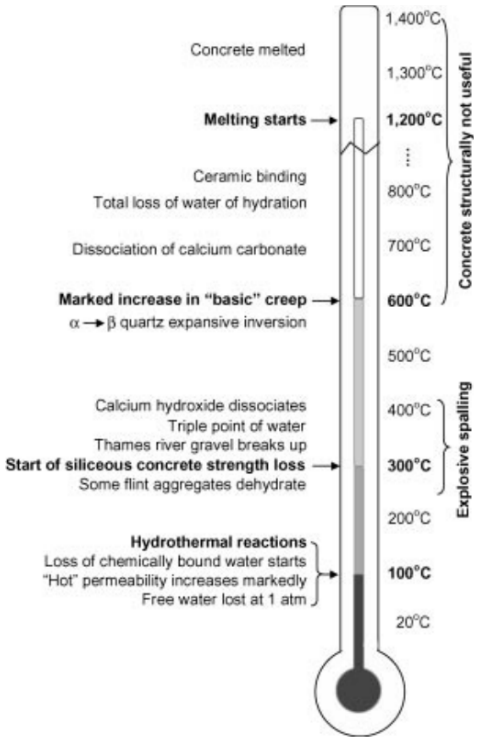

Figure 2 Physiochemical changes of concrete at elevated temperatures (Khoury, 2000).

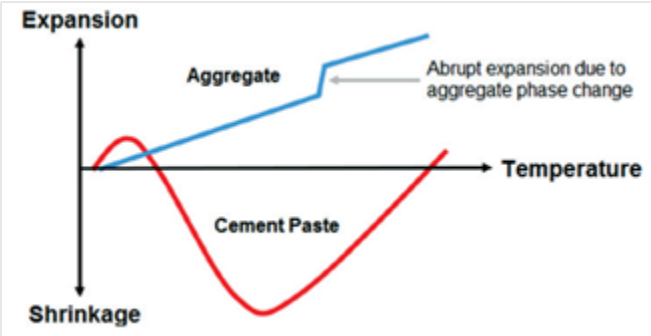

Figure 3 Thermal incompatibility between hydrated cement paste and aggregates (Fernandes et al., 2017).

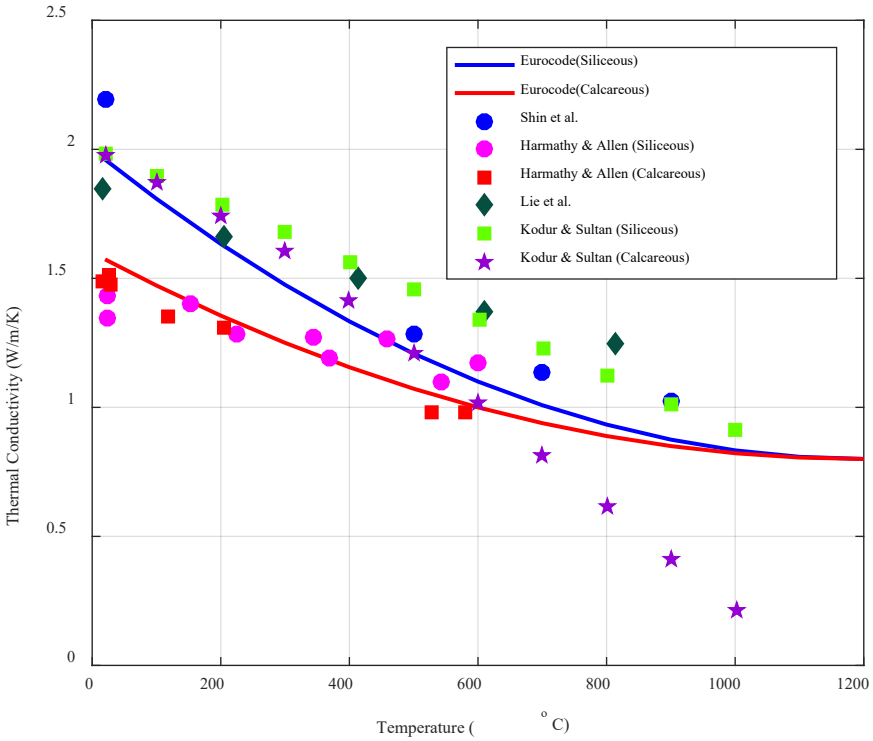

Figure 4 Variation of Thermal Conductivity

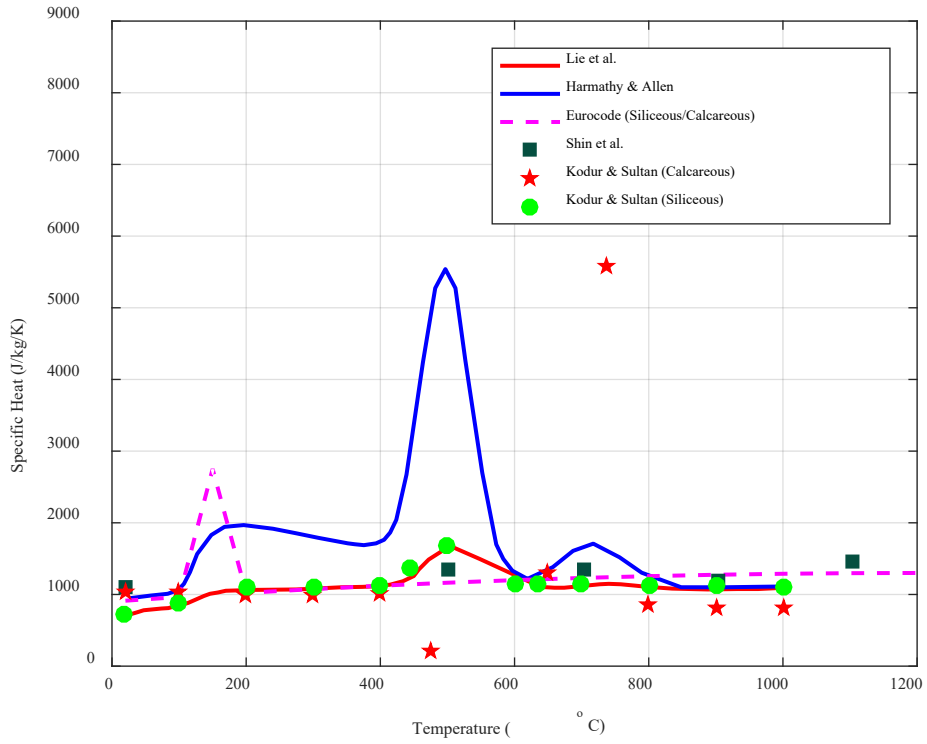

Figure 5 Specific Heat of Different types of Concrete

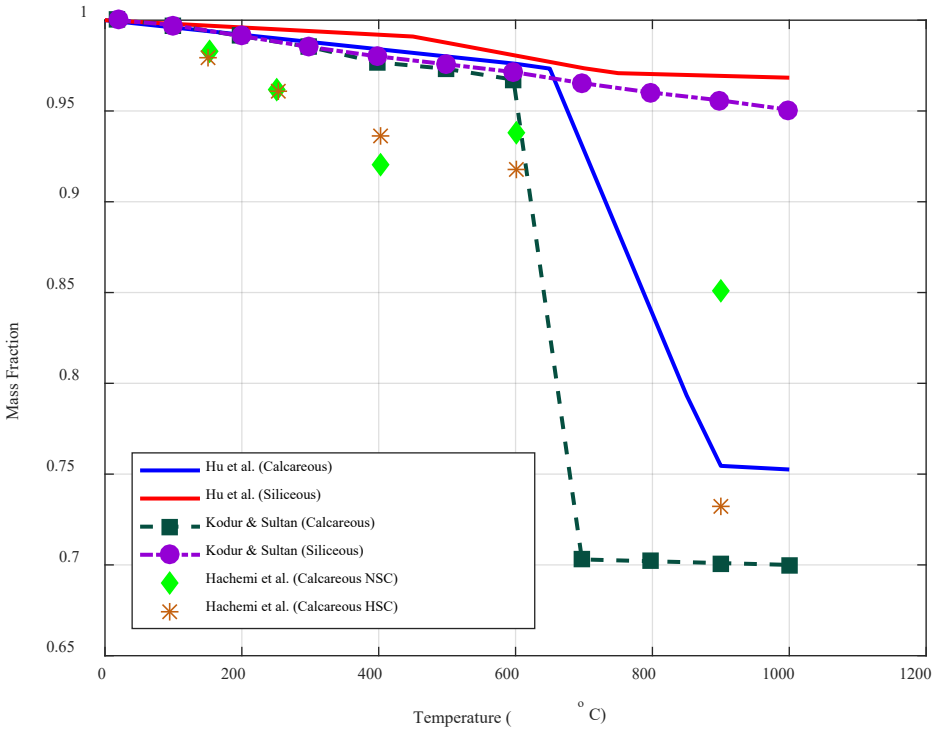

Figure 6 Mass Loss of Concrete vs Temperature

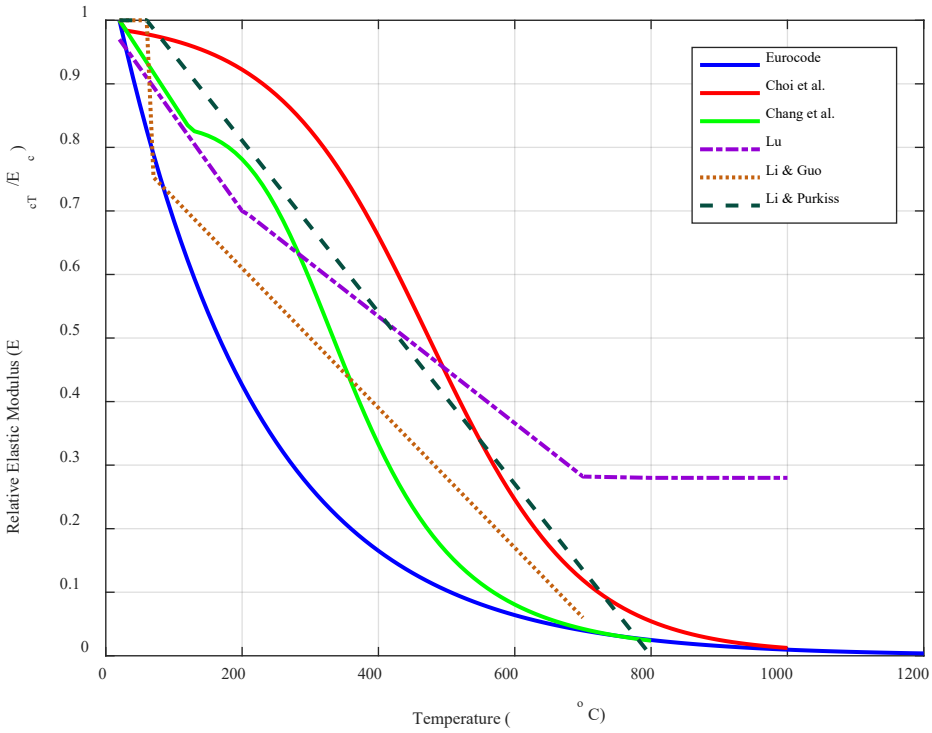

Figure 7 Variation of Elastic Modulus of Concrete with Temperature

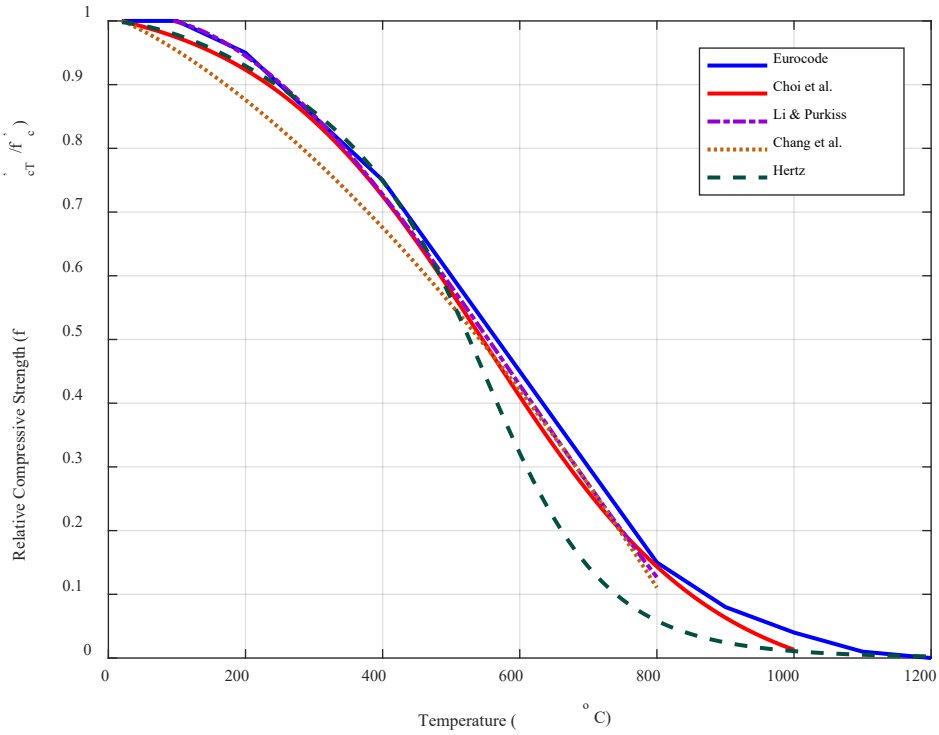

Figure 8 Variation of Compressive Strength of Concrete with Temperature

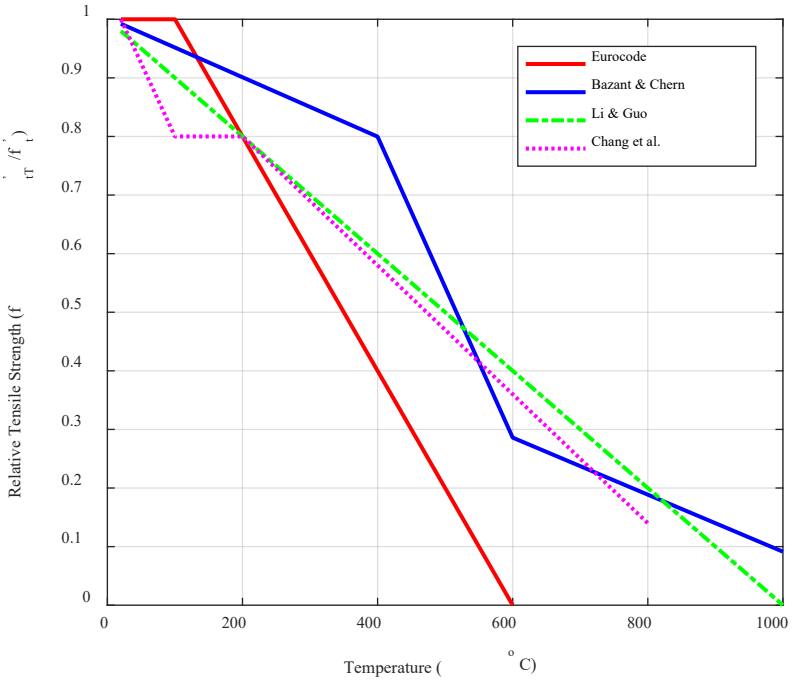

Figure 9 Relative Tensile Strength of Concrete with Temperature

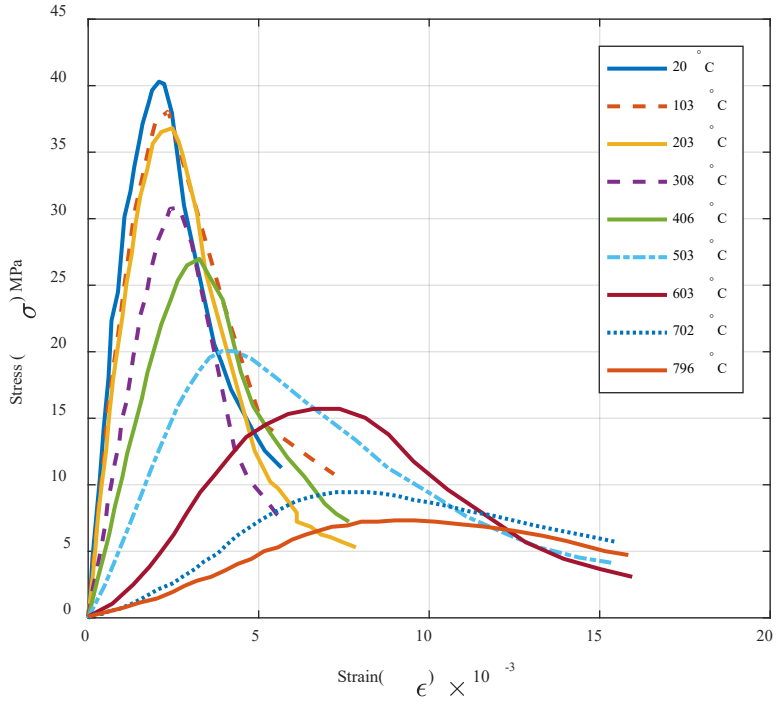

Figure 10 Experimental Stress Strain behavior of 40 MPa Concrete at Elevated Temperatures (Y. F. Chang et al., 2006)

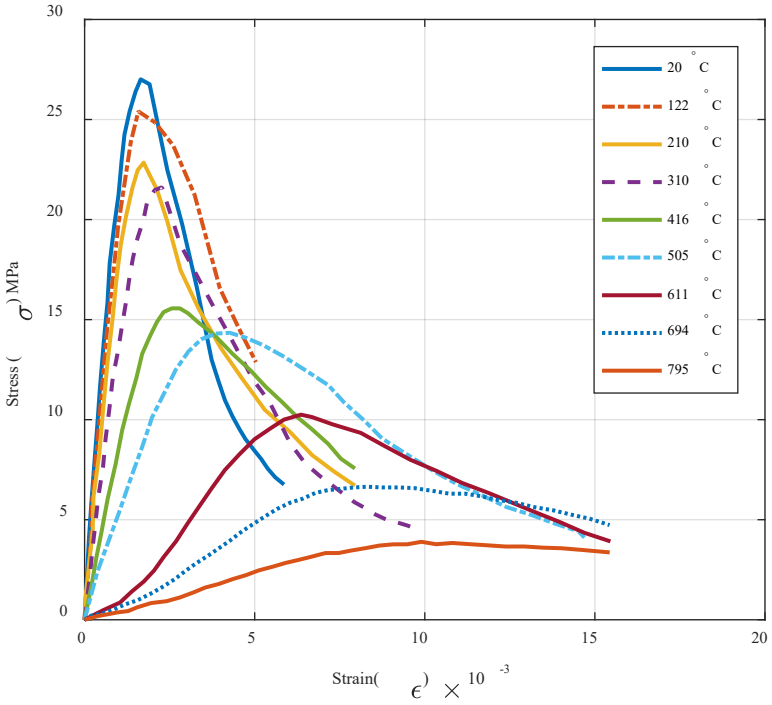

Figure 11 Experimental Stress Strain behavior of 26 MPa Concrete at Elevated Temperatures (Y. F. Chang et al., 2006)

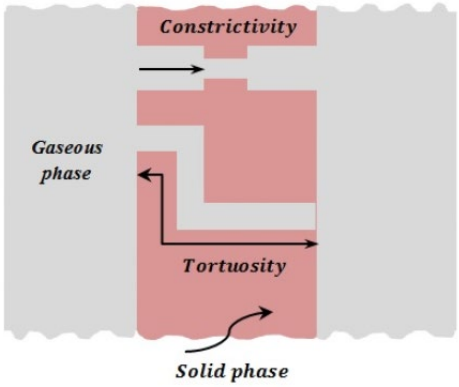

Figure 12 Schematic of tortuosity and constrictivity (Fadul, 2017)